J Nanostruct 12(1): 213-223, Winter 2022

RESEARCH PAPER

Graphene Oxide/Chitosan Based Impedimetric Aptasensor Along with an Ester Linker for the Detection of Tetracycline

Ali Benvidi *, *Maryam Nikmanesh, Marzieh Dehghan Tezerjani*

Department of Chemistry, Faculty of Science, Yazd, Yazd, I. R. Iran

ARTICLE INFO

Article History:
Received 21 September 2021
Accepted 24 December 2021
Published 01 January 2022

Keywords:
Graphene oxide/chitosan nano composite
Immobilization
Impedimetric aptasensor
Tetracycline

ABSTRACT

In the present study, an impedimetric aptasensor was designed based on a glassy carbon modified with nano composite of graphene oxide-chitosan along with 1-Pyrenebutyric acid–N-hydroxysuccinimide ester (Pry) linker to detect tetracycline antibiotic. After the modification of the electrode surface, the aptamer strands were immobilized on it, and it was then used for determination tetracycline concentration. Under optimum conditions, aptamer revealed a linear range of 1.0×10^{-15} - 3.2×10^{-7} with a detection limit of 3.2×10^{-16} M for determination of tetracycline. Some advantages of this biosensor are being highly selective and sensitive for detection of tetracycline, not expensive and easy preparation. Also, this designed aptasensor was applied in the real samples of drug and serum solutions successfully. Moreover, it can be implied that this creates a basis for improvement in graphene oxide-based impedimetric biosensors.

How to cite this article
Benvidi A, Nikmanesh M, Dehghan Tezerjani M. Graphene Oxide/Chitosan Based Impedimetric Aptasensor Along with an Ester Linker for the Detection of Tetracycline. J Nanostruct, 2022; 12(1):213-223. DOI: 10.22052/JNS.2022.01.020

INTRODUCTION

Nowadays, antibiotics have a key role in human health. Tetracycline is known as an antibiotic which reduces affinity for prokaryotic tRNA by strong binding on the 30S ribosomal subunit [1,2]. Tetracyclines are a group of broad-spectrum antibiotics containing four condensed aromatic rings. According to their sources, tetracyclines can be divided into two types, and the most commonly used tetracyclines are oxytetracycline (OTC), doxycycline (DOX), and tetracycline (TET). This antibiotic has been used for animals as growth promoters [3,4]. Tetracyclines are also found in food products, and it is known to be hepatotoxic agent [5,6].

Up to now, lots of methods have been reported by researchers for the detection of tetracycline antibiotics in food products, pharmaceutical preparations and water [5,7,8]. The electrochemical technologies have attracted considerable attention due to some advantages like ease in operation, high specificity and sensitivity, and amenability to automation for determination of TET as analyte [7-11]. But these sensitive detection techniques for tetracycline have some limitations like being time-consuming, expensive, and labor intensive.

As known, aptamers are single-stranded RNA or DNA oligonucleotides screened from synthetic DNA/RNA libraries using SELEX procedure (a systematic evolution of ligands by exponential enrichment) with high affinity and specific recognition to their target [12]. Some advantages of aptamers are better target versatility, stronger affinity, more stability, and resistant toward denaturation and degradation [13,14]. Azadbakht

* *Corresponding Author Email: abenvidi@yazd.ac.ir*

et al. designed an impedimetric aptasensor based on functionalized carbon nanotubes and prussian blue as labels [15].

Attaching biological recognition elements to nanomaterials leads to designing novel biosensors. Chitosan (Chit) as the most interesting biopolymer matrix for the immobilization of biological sensing elements due to lots of amino groups, good biocompatibility, and provides excellent film-forming ability and good adhesion acts. But owing to its non-conductive property, it is necessary to improve its conductivity. To attain this aim, many nanomaterials have been incorporated such as conducting polymer, metal nanoparticles, carbon nano tubes (CNTs) and graphene (GP). Among these, GP has been paid more attention for its low cost and large active surface area per volume ratio [16,17]. 1-Pyrenebutyric acid–N-hydroxysuccinimide (Pyr) ester as a scaffold molecule contains an anchor group and a terminal group. The hydrophobic p system group, pyreny moiety, has strong affinity with the basal plane of GO via p-stacking [18]. The succinimidyl ester group is highly reactive to nucleophilic substitution by primary and secondary amines that exist on protein surface [19]. Because of the specific structure of Pyren, it is one of the linkers which can be used for fabrication of some electro - chemical biosensors [20]. In the present study, the impedance method (EIS) was applied for the experiments as there is no need to additional biomolecule markers; the high sensitive, and is capable to separate the surface binding events from the solution resistance in spite of lower selectivity than some other methods [21,22].

Following the previous studies, [23-27] in this research, an electrochemical aptasensor was developed for the detection of tetracycline based on a modified glassy carbon electrode with graphene oxide/chitosan along with the linker of 1-Pyrenebutyric acid–N-hydroxy succin imide ester (Pyr). Some advantages of this include using 1-Pyrenebutyric acid–N-hydroxy succin imide ester (Pyr) as a linker agent and consequently preparing a more suitable platform for aptamer immobilization; beside, there is no need to use NHS/EDC during the fabrication steps of the aptasensor and the application of the constructed sensor for real samples. It is noticeable that the Apta/Pyr/Chit/GO/GCE aptasensor was successfully applied for TET detection in real samples of serum and tablet.

MATERIALS AND METHODS

Chemicals

All oligonucleotides were prepared from Bioneer Company (Korea) and the base sequence was as follows:

76 mer, 5'-NH2-CGT ACG GAA TTC GCT AGC CCC CCG GCA GGC CAC GGC TTG GGT TGG TCC CAC TGC GCG TGG ATC CGA GCT CCA CGT G- 3' (Mw. (23545.6), Tm (98.9 ˚C))[27,28].

Chemical reagents including sodium dihydrogen phosphate, disodium hydrogen phosphate, 1- pyrenebutyric acid-N- hydroxysuccinimide ester (Pyr), Tween 20 (Polyoxyethylenesorbitan monolaurate), potassium ferrocyanide, potassium ferricyanide, hydrochlorides of tetracycline (TET), oxy tetracycline (OTC), doxycycline (DOX), and diclofenac sodium salt (DCF), chitosan (Chit), graphite and salts for buffer solution contain NaCl, $MgCl_2$, KCl, $CaCl_2$ and other chemicals were purchased from Merck or Sigma companies in analytical grades.

Instrumentation and Electrochemical Experiments

A potentiostat/galvanostat Autolab model PGSTAT 30 (Eco Chemic, Utrecht, Netherlands) and a NOVA 1.7 software (25 ± 1 °C) were used for the electrochemical measurements. A three-electrode system containing the Apta/Pyr/Chit/GO/GCE as a working electrode, an Ag/AgCl (KCl 1.0 M) as a reference, and a platinum wire as a counter electrode was used. Cleaning the surface of electrodes was performed using an ultrasound cleaner VGT-QTP 1730 in which mechanical-ultrasonic waves (20-40 KHz) were produced. A Metrohm model 691 pH/mV meter was used for pH measurements. Charge transfer resistance (R_{ct}) and the differential charge transfer resistance (ΔR_{ct}) were considered as the analytical markers. The SEM was performed respectively with a TESCAN instrument model VEGA3. The electrochemical measurements were tested in a 0.1 M KCl solution containing the redox couples of $K_4Fe(CN)_6$ (0.5 mM) and $K_3Fe(CN)_6$ (0.5 mM). A binding buffer containing 20 mM tris-HCl (pH = 7.6) with 100 mM HCl, 2 mM $MgCl_2$, 5 mM KCl, 1 mM $CaCl_2$ was used [29]. The DPV conditions included the potential range of 0.05 V to 0.6 V with pulse amplitude of 50 mV and the scan rate of 100 mVs^{-1}.

Graphene Oxide /Chitosan Nano Composite Preparation

Nanosheets of graphene oxide were prepared

by using an improved method [30]. 0.0188 g, and 0.00376 g of graphene oxide and chitosan, respectively, were weighed and added to 1 mL of double-distilled water (the constant percentage of 80% w/w was used as the optimal percentage of GO in the Chit/GO composite). The prepared suspension was placed in an ultrasonic bath for 5 min, and then the obtained suspension was used for the electrode surface modification.

Impedimetric Aptasensor Construction

The fabrication of this aptasensor contains the following processes: i) polishing the surface of the glassy carbon electrode using 0.05 µm alumina slurry and washing with anhydrous alcohol and water solutions by ultra-sonication for 30 min, respectively; ii) the electrode surface modification by placing 20 µL homogeneously dispersed solution of graphene oxide (0.0188 g mL^{-1}) /chitosan (0.0037 g mL^{-1}) nano composite on it and drying under ambient condition. iii) the creation of linkage between GCE modified surface and aptamer oligonucleotide strands using the 1- pyrenebutyric acid-N- hydroxysuccinimide ester (Pyr) solution for 30 min [21]; iv) placing the aptamer solution (0.3 µM, 20 µL) on the electrode surface for 6 h in a wet chamber to obtain Anti-TET/Pyr/GO/Chit/GCE. Also, the pretreatment of aptamer was performed as follows: i) denaturation of aptamer at 90 °C for 10 min, ii) cooling at 4 °C for 15 min and iii) placing it at 25 C for 5 min. This Anti-TET/Pyr/Chit/GO/GCE electrode was immersed in ethanolamine for 1 h.

RESULTS AND DISCUSSION

The Anti-TET /Pyr / Chit / GO / GCE aptasensor fabrication

In the current study, the aptasensor was constructed attaching an aptamer to the modified glassy carbon electrode with graphene oxide nanosheets and chitosan composite. Also, the covalent crosslinking for chitosan caused the formation of hydrogels with a permanent network structure, since irreversible chemical links are formed. Then, 20 µL of Pyr solution (1 µmol L^{-1}) was dropped on the surface of modified for 30 min. At the last step, the selected aptamer containing 76-base sequences [27] as a target was introduced to the Pyr/Chit/GO/GCE surface. Graphene oxide nanosheets and chitosan composite were applied as an amplifier of peak current changes for TET binding due to the unique properties. The fabrication steps of the designed aptasensors were revealed in Fig. 1.

The Morphology Study of the Designed Aptasensor Surface Using SEM Technique

The surface morphology of GCE, GO/GCE and Chit/GO/GCE was investigated through scanning electron microscopy (SEM) technique. As shown in Fig. 2A, the SEM of bare GCE has a surface without any prouse compared to the SEM of GO/GCE (Fig. 2B), which contains nanosheets of graphene oxide with a nest-like porous structure. Fig. 2C reveals the SEM of the surface of modified glassy carbon with graphene oxide nanosheets and chitosan composite (Chit/GO/GCE) containing nanosheets of graphene oxide that have sharp edges and nanoparticles of chitosan which can be resulted in preparation of a large surface area. This, consequently, leads to preparing a suitable activity toward the aptamer.

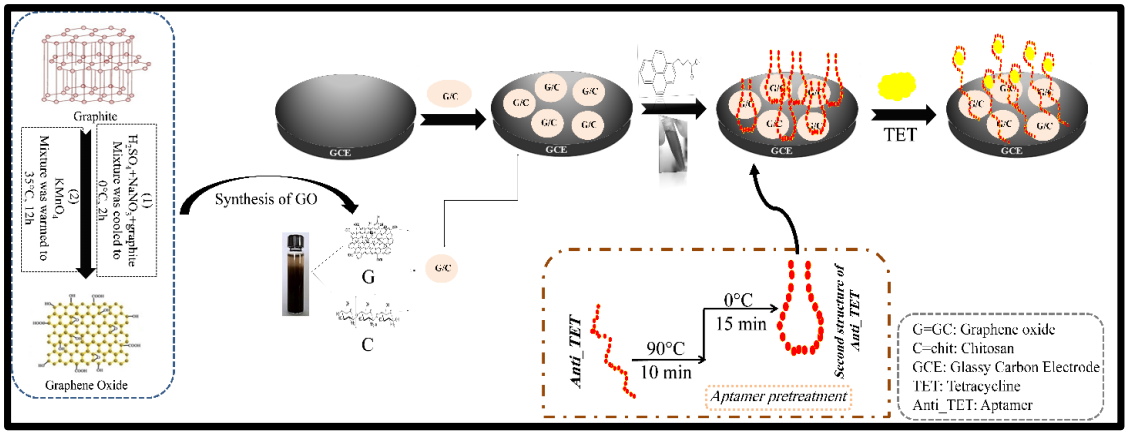

Fig. 1. A schematic representation of Anti-TET/Pyr/ GO/Chit/ GCE aptasensor construction.

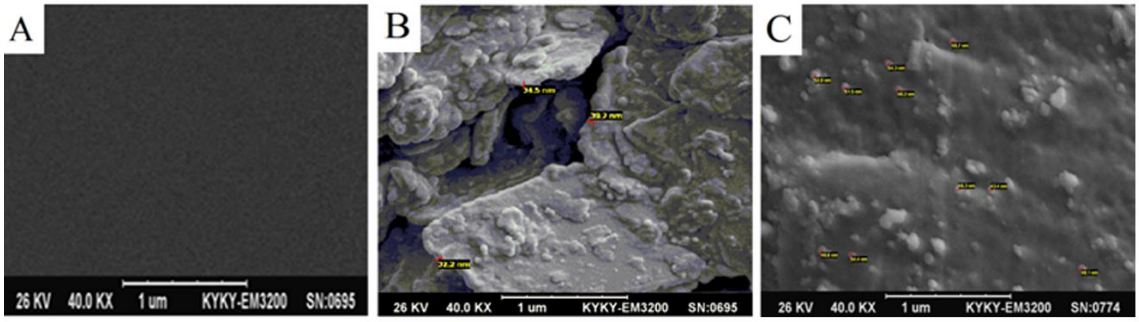

Fig. 2. The SEM images of A) bare GCE, B) GO/GCE and C) Chit/GO/GCE.

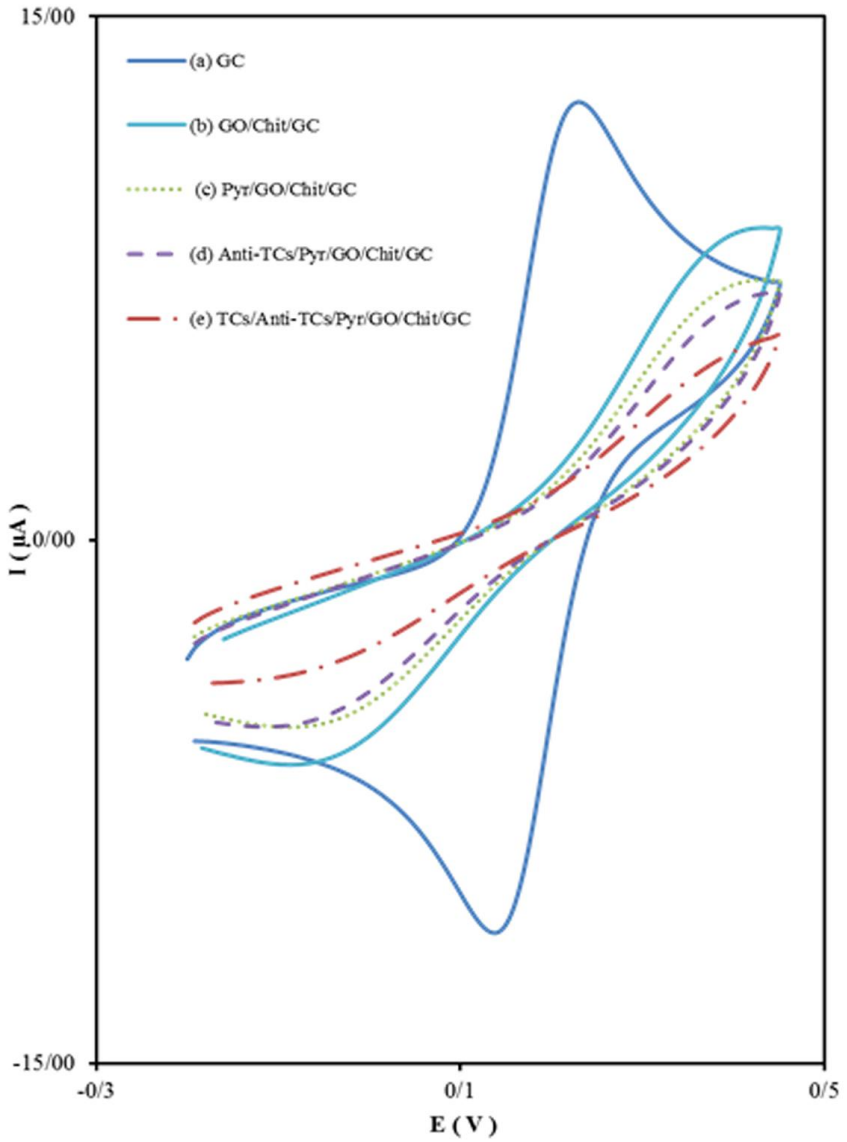

Fig. 3. The obtained CVs for 0.5 mM [Fe(CN)6]3−/4 and 0.1 M KCl at the surface of (a) bare GCE, (b) Pyr/Chit/GO/GCE, (c) Anti-TET/Pyr/GO/Chit/GCE (e) TET/Anti-TET/Pyr/GO/Chit/GCE (scan rate 100 mVs^{-1}).

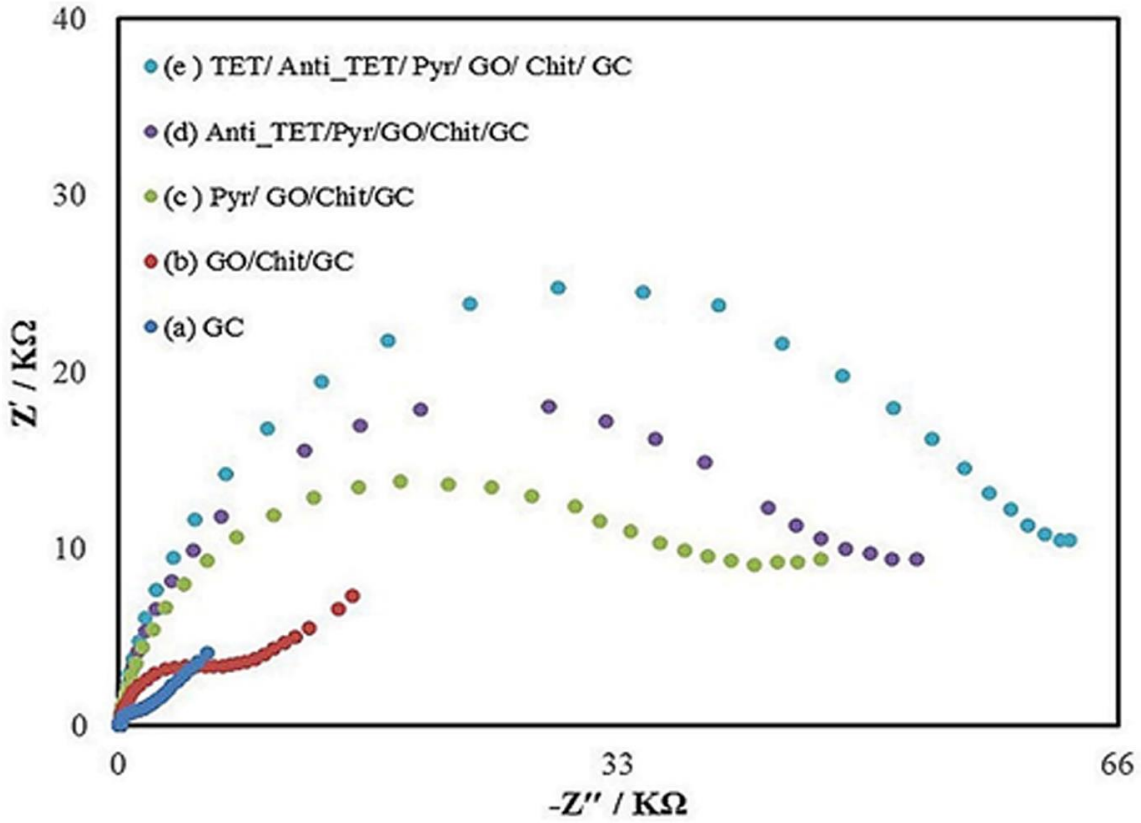

Fig. 4. The impedance (EIS) signals obtained for (a) bare GCE, (b) Pyr/Chit/GO/GCE, (c) Anti-TET /Pyr/GO/Chit/GCE (e) TET/Anti-TET/ Pyr/GO/Chit/GCE electrode, EIS conditions: initial ac potential of 5 mV, the frequency ranges of 10 kHz to 0.1 Hz).

Characterization of the Constructed Aptasensor y EIS and CV Techniques

The construction of the aptasensor was tested by electrochemical techniques of cyclic voltammetry and impedance. Fig. 3 indicates the obtained cyclic voltammograms of different electrodes (in $[Fe(CN)_6]^{3-/4-}$ solution (0.5 mM) and the scan rate of 100 mV s^{-1}). The curves a and b of this figure indicate that the peak current (i_p) is decreased by the modification of GCE with graphene oxide nano sheets and chitosan suspension. This can be related to the reduction of conductivity because of a surface electrode coverage with a composite of biomolecule of chitosan and graphene oxide nano sheets. As shown in curve c, by addition of Pyr to the surface of Chit/GO/GCE, the peak current is decreased due to preventing $[Fe(CN)6]^{3-/4-}$ ions from reaching to the surface of electrode. After the immobilization processes of the aptamer solution (0.3 µM) on the surface of Pyr/Chit/GO/GCE, the current value is decreased because the effective area and active sites for electron transfer is reduced (see curve d) [30]. Through TET antibiotic to Anti-TET/Pyr/Chit/GO/GCE, the CV response is decreased. This phenomenon can be related to the interaction of aptamer with TET which can lead to blocking the diffusion of $[Fe(CN)_6]^{3-/4-}$ towards the surface of electrode (curve e) [28].

Fig. 4 shows the EIS signals for modification steps. Curves a and b in this figure indicates that by the modification of the bare glassy carbon electrode with graphene oxide nanosheets and chitosan, R_{ct} value is enhanced compared to bare GCE due to increase in the oxygen groups and non-conductive property of chitosan at the surface of Pyr/Chit/GO/GCE electrode. As indicated in curve c, by the addition of Pyr to the surface of modified glassy carbon with graphene oxide and chitosan, the peak current is decreased. As shown in curve d, the semicircle diameter is increased by aptamer immobilization on the Pyr/Chit/GO/GCE surface which can be related to formation of an insulating DNA layer on the electrode surface [30]. At last, the interaction of aptamer and TET causes

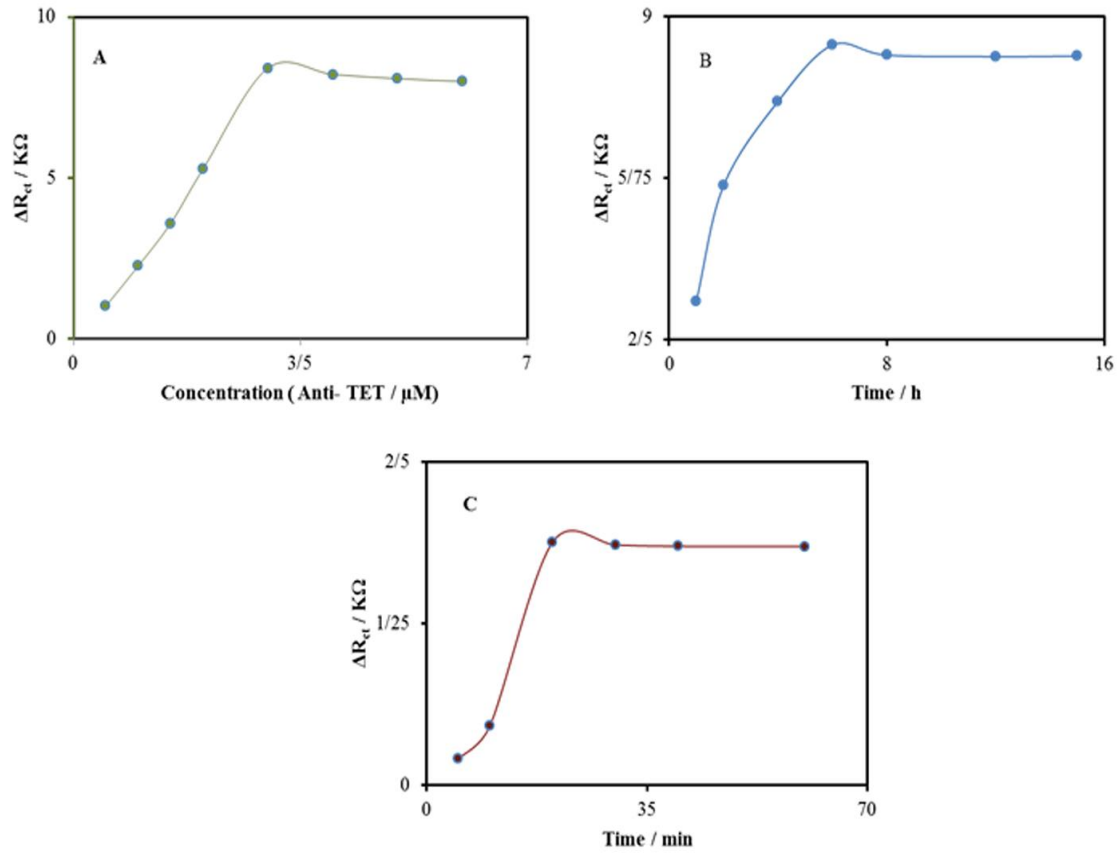

Fig. 5. A) Optimization of the influence of anti-TET concentration at 25 °C, B) Effect of immobilization time of anti-TET (3.0 µ mol L^{-1}), C) Optimization of influence of TET reaction time.

an increase in the diameter of the semicircle in the impedance spectrum as the result of more repulsion between negatively charge of Apta/TET complex and $[Fe(CN)_6]^{3-/4-}$ anions (see curve e). According to the obtained results in Fig. 3 and Fig. 4, the EIS and CV results have a good agreement, which implies that the fabrication of Anti-TET/Pyr/Chit/GO/GCE aptasensor was done well.

The Experimental Parameters Optimization

The time and concentration of aptamer are important factors for sufficient reaction of the designed aptasensor (Anti-TET/Pyr/Chit/GO/GCE) with target; consequently, they were optimized. The change of electron charge transfer resistance ($\Delta R_{ct} = (R_{ct})_{final} - (R_{ct})_{initial}$) was assumed as the measurement signal. The aptamer concentration was examined from 0.1 to 6 µmol L^{-1}. The results show that ΔR_{ct} values are increased from 1 µmol L^{-1} to 3.0 µmol L^{-1} and after that it will be constant. Which is probably due to the saturation of Chit/GO/GCE surface with aptamer. On the basis of these observations (Fig.5A), the concentration of 3.0 µmol $L^{-1}$was chosen as an optimum point and was applied for the experiments. The immobilization time of aptamer on the modified electrode was studied, too. The different times of aptamer (3.0 µ mol L^{-1}) immobilization on the electrode surface from 1 h to 15 h was examined. The optimum value of 6 h was obtained for the immobilization time of aptamer (Fig. 5B). After investigation of influence of aptamer concentration and immobilization time, another effective parameter (the detection time of TET antibiotic) was examined. The results indicated that ΔR_{ct} values increased when 10 µL of TET (1×10^{-8} mol L^{-1}) was introduced on the surface of electrode after 20 min, and then was stabilized (see Fig. 5C). It means that after 50 minutes, the obtained complex between aptamer and TET was saturated on the modified glassy carbon. Thus, 20 min was selected as the detection time of target (TET).

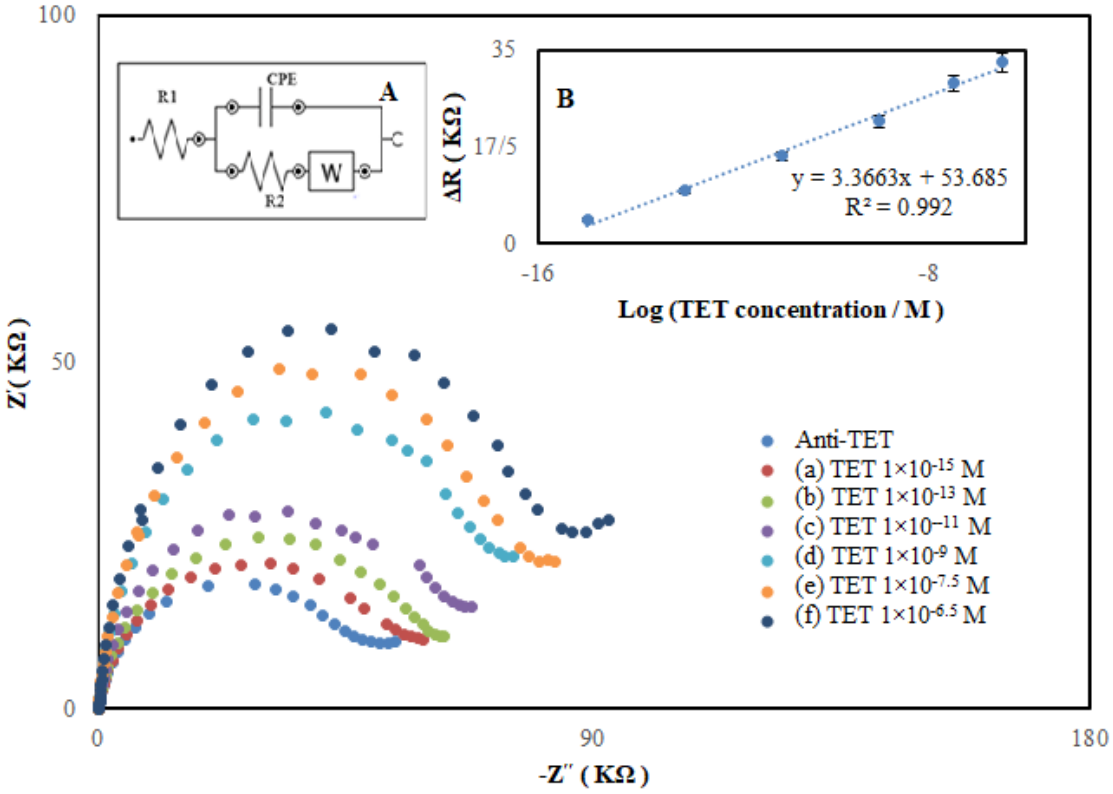

Fig. 6. The obtained Nyquist plots of Anti-TET/Pyr/GO/Chit/GCE aptasensor before and after hybridization with various TET concentrations (n=5). Inset A: the used equivalent circuit for impedance data (while R_1, W, CPE, R_2 (R_{ct}) parameters are the electrolyte resistance, Warburg impedance, a constant phase element and the electron transfer resistance, respectively), Inset B: the dependence of ΔR_{ct} versus the concentration of TET.

The Sensitivity Investigation by Impedance Technique (EIS)

Fig. 6 shows the obtained impedance signals which increased through different concentration of tetracycline on the Anti-TET/Pyr/GO/Chit/GCE surface. Used Randles equivalent circuit for EIS measurement is shown in the insertion A of this figure. In the present study, the electron transfers resistance (R_{ct}) process has occurred between the redox indicator solution and electrode surface, and R_{ct} can change with variation of target concentration. A calibration plot with a regression equation of ΔR_{ct} = 3.366 Log C (M) + 53.685 (R^2 = 0.992) was obtained. The linear range was from 1.0×10^{-15} mol L^{-1} to $1.0 \times 10^{-6.5}$ mol L^{-1} (inset B), and the detection limit based on 3_{sbl} was calculated to be 3.2×10^{-16} mol L^{-1}.

The Sensitivity Study by Voltammetry Technique (DPV)

To study the sensitivity of the constructed aptasensor, the differential pulse voltammetry (DPV) technique was applied, too. The peak currents of $[Fe(CN)_6]^{3-/4-}$ versus potential values for different concentrations of antibiotic target were obtained (Fig. s1). The plotting of calculated ΔI versus different concentrations of tetracycline antibiotic on the surface of the designed aptasensor revealed a regression equation of ΔI = 0.0857 Log C (M) +1.2239 (R^2 =0.9947). The linear range of 1.0×10^{-13} mol L^{-1} to 3.2×10^{-8} mol L^{-1} and the detection limit of 3.1×10^{-14} mol L^{-1} (based on 3_{sb}) were obtained. Table 1 indicates the comparison of the Anti-TET/ Pyr / Chit / GO/ GCE aptasensor with other reported electrochemical aptasensors [27,29,31-34]. Based on Table 1, the constructed aptasensor has a low detection limit and wide linear range.

The Effect of Interference Species on the Designed Aptasensor

After sensitivity study of the fabricated aptasensor,

Table 1. The analytical performances of Anti-TET/ Pyr/ GO /Chit/GCE aptasensor compared to some reported aptasensors.

Aptasensor	Detection technique	Linear range (M)	Detection Limit (M)	Ref.
GO/GCE	EIS	1.0×10^{-13}-1.0×10^{-5}	2.9×10^{-14}	[27]
GCE	DPV	1.0×10^{-8}-5.0×10^{-5}	5.0×10^{-9}	[29]
SPGE	dc A	1.0×10^{-6}-5.0×10^{-4}	0.96×10^{-6}	[32]
PB-CS-GA	DPV	1.0×10^{-9}-1.0×10^{-2}	3.2×10^{-10}	[33]
GE	EIS	5.0×10^{-8}-5.0×10^{-5}	1.0×10^{-9}	[34]
Microplate	ELAA	3.16×10^{-8}-3.16×10^{-4}	2.1×10^{-8}	[35]
Pyr/GO/Chit /GCE	EIS	1.0×10^{-15} - 3.2×10^{-7}	3.2×10^{-16}	This research

Screen-printed gold electrode: SPGE, dc amperometry: dc A, PB-chitosan-glutar aldehyde: (PB-CS-GA), GE: gold electrode, Differential pulse voltammetry: DPV, Enzyme-Linked Aptamer Assay: ELAA, Graphene oxide: GO, Glassy carbon electrode: GCE.

it was essential to test its selectivity. To attain this aim, the effect of possible interferences on the detection of TET was examined. To perform the selectivity of the designed aptasensor, different antibiotics of oxytetracycline (OTC), and doxycycline (DOX) which have a similar structure with tetracycline and pain killer of diclofenac (DCF) with a different structure were tested. According to the obtained observations, only the tetracycline antibiotic reveals a high ΔR_{ct} (4.2 KΩ), and other drugs indicate a lower ΔR_{ct} compared to TET antibiotic. The obtained ΔR_{ct} for OTC, DOX and DCF were obtained 0.80, 0.50 and 0.10 kΩ, respectively (Fig. 7). It is noticeable that DCF with its non-similar structure shows the lowest ΔR_{ct} value (0.1 K) compared to other tested samples. Hence, due to these results, the fabricated aptasensor reveals a good selectivity for detection of tetracycline antibiotic.

Reproducibility and Stability of the Fabricated Aptasensor

Obviously, the ability of the designed sensor for denerating a reproducible surface is defined by reproducibility. For the reproducibility test of the Anti-TET/Pyr/GO/Chit/GCE aptasensor, four separated aptasensors were constructed in a day through similar conditions using impedance technique (EIS). The observations indicated a relative standard deviation of 4.05% (n=4) for ΔR_{ct} while ΔR_{ct} is $(R_{ct})_{\text{after interaction}}$-$(R_{ct})_{\text{before interaction}}$. The second parameter to be tested, was the aptasensor stability. The stability of the Anti-TET/Pyr/GO/Chit/GCE aptasensor was investigated in three days. The fabricated aptasensor was stored in PBS (0.1 M, pH=7.4) at 4 °C. After three days the Anti-TET/Pyr/GO/Chit/GCE aptasensor was used for TET detection (1.0×10^{-8} mol L^{-1}). The results revealed that the ΔR_{ct} obtained about 91% of its initial response. According to these results, the reproducibility and stability of Anti-TET/Pyr/GO/Chit/GCE aptasensor can be reported to be suitable.

Analytical Figure of Merit

Due to the importance role of the designed aptasensor for determination of TET antibiotic in real sample, the fabricated aptasensor was tested in the drug and serum solutions. For the preparation of TET sample solution, the purchased

tetracycline tablets were ground (tablets of TET were prepared from local source). After grinding, 98 mg of the obtained powder was weighed and dissolved in 100 mL of PBS (pH = 7.6). The concentration of prepared solution was calculated using the labeled weight percent. To obtain different TET concentrations (1.0×10^{-12} mol L^{-1}, 1.0×10^{-10} mol L^{-1}), the initial prepared solution was diluted towards the TET calibration range. At last, Anti-TET/Pyr/GO/Chit/GCE electrode was tested for calculation of the concentration of TET (0.95 (±0.02) $\times 10^{-12}$ and1.08 (±0.02) $\times 10^{-10}$). The results revealed that the calculated t values of 2.4 and 2.3 are less than tabulated t value of 4.3 (the confidence level of 95%) which indicates a high potential of the fabricated aptasensor for TET determination in the drug sample (tablet solution) [35]. Also, the applicability of the constructed aptasensor was tested in the serum sample. To obtain this purpose, the serum solution was diluted with PBS and then two concentration of TET (1.0×10^{-11} mol L^{-1} and 1.0×10^{-7} mol L^{-1}) were spiked to serum solutions, individually. Anti- TET/Pyr/GO/Chit/GCE aptasensor was used for detection of

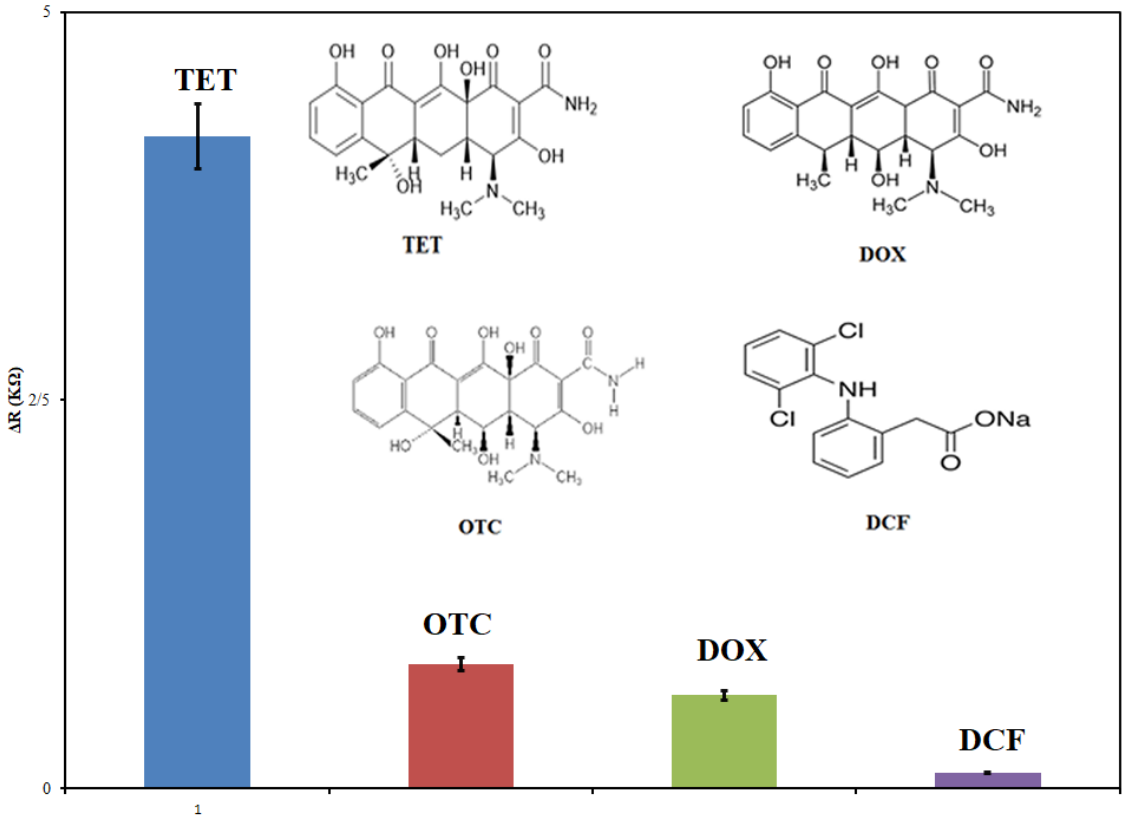

Fig. 7. Specificity test using the Anti-TCs/Pry/Chit/GO/GC aptasensor responses to different targets (1 µM) of TCs, OTC, DOX and DCF, inset: chemical structures of tetracycline (TCs), oxytetracycline (OTC), doxycycline (DOX), and diclofenac (DCF), (n=3).

Table 2. Antibiotic (TET) concentration determination in serum solution by the proposed method. (n=3)

Spiked value (M)	Found value (M)	Recovery (%)
1.0×10^{-11}	$0.97 (\pm 0.04) \times 10^{-11}$	97
1.0×10^{-7}	$0.98 (\pm 0.03) \times 10^{-7}$	98

the mentioned TET concentrations by using DPV technique. The obtained recovery percentages in Table 2 show that the proposed aptasensor has a suitable applicability for TET detection in serum solutions as well as drug sample.

CONCLUSION

In the present study, the fabrication of an aptasensor for tetracycline antibiotic detection based on a glassy carbon modified with graphene oxide nanosheets / chitosan composite and Pyr as a linker, is introduced. After the optimization of experimental conditions, a wide dynamic range and a low detection limit of 3.2×10^{-16} mol L^{-1} for detection of TET were obtained by impedance (EIS) technique. Some advantages of this designed aptasensor are the modification of electrode surface using composite of graphene oxide nanosheets and chitosan; using pyren as a linker that leads to a decreasing in electrode preparation, its good sensitivity, suitable selectivity, stability, and applicability for tetracycline antibiotic detection in real samples (tablet and serum solutions).

ACKNOWLEDGEMENTS

The current study was supoorted by Yazd University Research Council, Iran.

CONFLICT OF INTEREST

The authors declare that there is no conflict of interests regarding the publication of this manuscript.

REFRENCES

1. Epe B, Woolley P, Hornig H. Competition between tetracycline and tRNA at both P and A sites of the ribosome of Escherichia coli. FEBS Lett. 1987;213(2):443-447.
2. Spahn CMT, Prescott CD. Throwing a spanner in the works: antibiotics and the translation apparatus. J Mol Med. 1996;74(8):423-439.
3. Hu X-C, Hu J-G, Sun J, Li G-H. Mesoporous Tungsten Carbide Supported Pt and Their Electro Catalytic Activity for Methanol Electro-oxidation. Journal of Inorganic Materials. 2013;28(12):1286-1290.
4. Oka H, Ito Y, Goto T, Minami T, Yamamoto I, Matsumoto H, et al. Survey of Residual Tetracycline Antibiotics and Sulfa Drugs in Kidneys of Diseased Animals in the Aichi Prefecture, Japan (1995–1999). J AOAC Int. 2003;86(3):494-500.
5. Zhao R, Wang Z, Yang Y, Xing X, Zou T, Wang Z, et al. Raspberry-like SnO_2 hollow nanostructure as a high response sensing material of gas sensor toward n-butanol gas. Journal of Physics and Chemistry of Solids. 2018;120:173-182.
6. Gwee MCE. Can tetracycline-induced fatty liver in pregnancy be attributed to choline deficiency? Med Hypotheses. 1982;9(2):157-162.
7. Monser L, Darghouth F. Rapid liquid chromatographic method for simultaneous determination of tetracyclines antibiotics and 6-Epi-doxycycline in pharmaceutical products using porous graphitic carbon column. Journal of Pharmaceutical and Biomedical Analysis. 2000;23(2-3):353-362.
8. Yang X-Q, Yang C-X, Yan X-P. Zeolite imidazolate framework-8 as sorbent for on-line solid-phase extraction coupled with high-performance liquid chromatography for the determination of tetracyclines in water and milk samples. Journal of Chromatography A. 2013;1304:28-33.
9. Jalink M, Ge Z, Liu C, Björkholm M, Gruber A, Xu D. Human normal T lymphocytes and lymphoid cell lines do express alternative splicing variants of human telomerase reverse transcriptase (hTERT) mRNA. Biochemical and Biophysical Research Communications. 2007;353(4):999-1003.
10. Vega D, Agüí L, González-Cortés A, Yáñez-Sedeño P, Pingarrón JM. Voltammetry and amperometric detection of tetracyclines at multi-wall carbon nanotube modified electrodes. Analytical and Bioanalytical Chemistry. 2007;389(3):951-958.
11. Weber CC, Link N, Fux C, Zisch AH, Weber W, Fussenegger M. Broad-spectrum protein biosensors for class-specific detection of antibiotics. Biotechnology and Bioengineering. 2004;89(1):9-17.
12. Yang C, Lates V, Prieto-Simón B, Marty J-L, Yang X. Aptamer-DNAzyme hairpins for biosensing of Ochratoxin A. Biosensors and Bioelectronics. 2012;32(1):208-212.
13. Citartan M, Gopinath SCB, Tominaga J, Tan S-C, Tang T-H. Assays for aptamer-based platforms. Biosensors and Bioelectronics. 2012;34(1):1-11.
14. Fischer NO, Tarasow TM, Tok JBH. Aptasensors for biosecurity applications. Curr Opin Chem Biol. 2007;11(3):316-328.
15. Beiranvand S, Azadbakht A. Electrochemical switching with a DNA aptamer-based electrochemical sensor. Materials Science and Engineering: C. 2017;76:925-933.
16. Azadbakht A, Roushani M, Abbasi AR, Derikvand Z. Design and characterization of electrochemical dopamine–aptamer as convenient and integrated sensing platform. Anal Biochem. 2016;507:47-57.
17. Safaei-Ghomi J, Shahbazi-Alavi H, Nazemzadeh SH. Synthesis of Bis-Thiazolidinones Using Chitosan-attached Nano-$CuFe_2O_4$ as an Efficient and Retrievable Heterogeneous Catalyst. J Chin Chem Soc. 2017;64(10):1213-1219.
18. Roushani M, Sarabaegi M. Novel electrochemical sensor based on carbon nanodots/chitosan nanocomposite for the detection of tryptophan. Journal of the Iranian Chemical Society. 2015;12(10):1875-1882.
19. Xu Y, Bai H, Lu G, Li C, Shi G. Flexible Graphene Films via the Filtration of Water-Soluble Noncovalent Functionalized Graphene Sheets. Journal of the American Chemical Society. 2008;130(18):5856-5857.
20. Chen RJ, Zhang Y, Wang D, Dai H. Noncovalent Sidewall Functionalization of Single-Walled Carbon Nanotubes for Protein Immobilization. Journal of the American Chemical Society. 2001;123(16):3838-3839.
21. Jahanbani S, Benvidi A. A novel electrochemical DNA biosensor based on a modified magnetic bar carbon paste electrode with Fe_3O_4 NPs-reduced graphene oxide/PANHS nanocomposite. Materials Science and Engineering: C. 2016;68:1-8.
22. Benvidi A, Abbasi Z, Tezerjani MD, Banaei M, Zare HR, Molahosseini H, et al. A Highly Selective DNA Sensor Based

on Graphene Oxide-Silk Fibroin Composite and AuNPs as a Probe Oligonucleotide Immobilization Platform. Acta Chimica Slovenica. 2018:278-288.
23. Benvidi A, Rajabzadeh N, Molaye Zahedi H, Mazloum-Ardakani M, Heidari MM, Hosseinzadeh L. Simple and label-free detection of DNA hybridization on a modified graphene nanosheets electrode. Talanta. 2015;137:80-86.
24. Benvidi A, Tezerjani MD, Firouzabadi AD, Mazloum-Ardakani M, Moshtaghioun SM. Application of graphene oxide nanosheets as probe oligonucleotide immobilization platform for DNA sensing. Journal of the Iranian Chemical Society. 2016;13(11):2135-2142.
25. Benvidi A, Jahanbani S. Self-assembled monolayer of SH-DNA strand on a magnetic bar carbon paste electrode modified with Fe_3O_4@Ag nanoparticles for detection of breast cancer mutation. J Electroanal Chem. 2016;768:47-54.
26. Jahanbani S, Benvidi A. Comparison of two fabricated aptasensors based on modified carbon paste/oleic acid and magnetic bar carbon paste/Fe_3O_4@oleic acid nanoparticle electrodes for tetracycline detection. Biosensors and Bioelectronics. 2016;85:553-562.
27. Benvidi A, Tezerjani MD, Moshtaghiun SM, Mazloum-Ardakani M. An aptasensor for tetracycline using a glassy carbon modified with nanosheets of graphene oxide. Microchimica Acta. 2016;183(5):1797-1804.
28. Zhou L, Li D-J, Gai L, Wang J-P, Li Y-B. Electrochemical aptasensor for the detection of tetracycline with multi-walled carbon nanotubes amplification. Sensors Actuators B: Chem. 2012;162(1):201-208.
29. Hu Y, Li F, Bai X, Li D, Hua S, Wang K, et al. Label-free electrochemical impedance sensing of DNA hybridization based on functionalized graphene sheets. Chem Commun. 2011;47(6):1743-1745.
30. Marcano DC, Kosynkin DV, Berlin JM, Sinitskii A, Sun Z, Slesarev A, et al. Improved Synthesis of Graphene Oxide. ACS Nano. 2010;4(8):4806-4814.
31. Masawat P, Slater JM. The determination of tetracycline residues in food using a disposable screen-printed gold electrode (SPGE). Sensors Actuators B: Chem. 2007;124(1):127-132.
32. Shen G, Guo Y, Sun X, Wang X. Electrochemical Aptasensor Based on Prussian Blue-Chitosan-Glutaraldehyde for the Sensitive Determination of Tetracycline. Nano-Micro Letters. 2014;6(2):143-152.
33. Chen D, Yao D, Xie C, Liu D. Development of an aptasensor for electrochemical detection of tetracycline. Food Control. 2014;42:109-115.
34. Mazloum-Ardakani M, Barazesh B, Khoshroo A, Moshtaghiun M, Sheikhha MH. A new composite consisting of electrosynthesized conducting polymers, graphene sheets and biosynthesized gold nanoparticles for biosensing acute lymphoblastic leukemia. Bioelectrochemistry. 2018;121:38-45.
35. Miller JC, Miller JN. Basic statistical methods for analytical chemistry. Part I. Statistics of repeated measurements. A review. The Analyst. 1988;113(9):1351.